Morphological and electrophysiological changes in intratelencephalic-type pyramidal neurons in the motor cortex of a rat model of levodopa-induced dyskinesia

（レボドパ誘発ジスキネジアモデルラット運動皮質錐体神経細胞における形態学的・電気生理学的変化）

申 請 者　　弘前大学大学院医学研究科
脳神経科学領域神経生理学講座

氏 名　　上野　達哉

指導教授　　上野　伸哉

Abstract

Levodopa-induced dyskinesia (LID) is a major complication of long-term dopamine replacement therapy for Parkinson's disease, and becomes increasingly problematic in the advanced stage of the disease. Although the cause of LID still remains unclear, there is accumulating evidence from animal experiments that it results from maladaptive plasticity, resulting in supersensitive excitatory transmission at corticostriatal synapses. Recent work using transcranial magnetic stimulation suggests that the motor cortex displays the same supersensitivity in Parkinson's disease patients with LID. To date, the cellular mechanisms underlying the abnormal cortical plasticity have not been examined. The morphology of the dendritic spines has a strong relationship to synaptic plasticity. Therefore, we explored the spine morphology of pyramidal neurons in the motor cortex in a rat model of LID. We used control rats, 6-hydroxydopamine-lesioned rats (a model of Parkinson's disease), 6-hydroxydopamine-lesioned rats chronically treated with levodopa (a model of LID), and control rats chronically treated with levodopa. Because the direct pathway of the basal ganglia plays a central role in the development of LID, we quantified the density and size of dendritic spines in intratelencephalic (IT)-type pyramidal neurons in M1 cortex that project to the striatal medium spiny neurons in the direct pathway. The spine density was not different among the four groups. In contrast, spine size became enlarged in the Parkinson's disease and LID rat models. The enlargement was significantly greater in the LID model than in the Parkinson's disease model. This enlargement of the spines suggests that IT-type pyramidal neurons acquire supersensitivity to excitatory stimuli. To confirm this possibility, we monitored miniature excitatory postsynaptic currents (mEPSCs) in the IT-type pyramidal neurons in M1 cortex using whole-cell patch clamp. The amplitude of the mEPSCs was significantly increased in the LID model compared with the control. This indicates that the IT-type pyramidal neurons become hyperexcited in the LID model, paralleling the enlargement of spines. Thus, spine enlargement and the resultant hyperexcitability of IT-type

pyramidal neurons in M1 cortex might contribute to the abnormal cortical neuronal plasticity in LID.

Highlights

- We examined dendritic spine morphology in intratelencephalic-type corticostriatal neurons in M1 of a rats with levodopa-induced dyskinesia.
- Dendritic spines in intratelencephalic-type corticostriatal neurons in M1 became enlarged.
- The amplitude of miniature excitatory postsynaptic currents in intratelencephalic-type corticostriatal neurons in M1 was increased.
- Intratelencephalic-type corticostriatal neurons in M1 become supersensitive in levodopa-induced dyskinesia.
- Spine enlargement and hyperexcitability in intratelencephalic-type corticostriatal neurons in M1 may be linked to development of dyskinesia.

Introduction

Oral L-3,4-dihydroxyphenylalanine (levodopa, L-DOPA) replacement therapy remains the most effective strategy for the symptomatic relief of Parkinson's disease (PD). However, chronic levodopa treatment is often complicated by a variety of involuntary movements, termed levodopa-induced dyskinesia (LID), which represent a major limitation in the treatment of PD (Fabbrini et al., 2007). LID mainly develops in response to activation of sensitized D1 receptors on medium spiny neurons in the direct striatonigral pathway (Feyder et al., 2011). Indeed, corticostriatal synapses in an LID model have been shown to exhibit abnormalities in synaptic plasticity (Picconi et al., 2003, 2008, 2011; Belujon et al., 2010). The corticostriatal synapse in this model lacks depotentiation after induction of long-term potentiation (LTP) (Picconi et al., 2003). Depotentiation leads to a resetting of corticostriatal synapses, to avoid synaptic saturation and is implicated in the mechanisms of physiological *forgetting*. Consequently, the absence of depotentiation might result in the storage of unessential motor information (Picconi et al., 2011). In addition, it has been shown that induction of long-term depression (LTD) is also lost in the dyskinetic model (Picconi et al., 2011). Thus, corticostriatal synapses appear to be electrophysiologically supersensitive in dyskinesia, and dyskinetic movements might be induced by changes in the molecular mechanisms regulating corticostriatal excitatory synaptic transmission (Picconi et al., 2011).

Direct investigation of corticostriatal plasticity in humans is not currently possible. Instead, abnormal neuroplasticity in patients with PD has been identified at the level of the motor cortex using transcranial magnetic stimulation (TMS) (Rothwell, 2007). Using this approach, PD patients with LID exhibit a lack of depotentiation-like cortical plasticity (Huang et al., 2012). Levodopa fails to effectively normalize the excitability of inhibitory systems and does not restore motor cortical plasticity in PD patients with dyskinesia, in contrast to its effects in PD patients without dyskinesia (Morgante et al., 2006). The electrophysiological changes in PD patients with LID are similar to those at corticostriatal

synapse of the LID model (Picconi et al., 2003, 2008, 2011; Belujon et al., 2010). It has been shown that abnormal motor cortical plasticity may arise from a loss of dopaminergic terminals in the primary motor cortex (M1) (Luft and Schwarz, 2009). Thus, abnormal synaptic plasticity, resulting in an increase in excitability to glutamate, occurs in the motor cortex of PD patients with LID, a structure that receives indirect inputs from the basal ganglia. However, the cellular mechanisms underlying the hyperexcitability of the motor cortex remain to be determined.

Dendritic spines form the postsynaptic compartment of the majority of excitatory glutamatergic synapses in the brain. The morphological properties of dendritic spines are intimately linked with synaptic functions; i.e., changes in synaptic plasticity are often accompanied by changes in spine size (Kasai et al., 2010a, 2010b). Accordingly, morphological examinations of dendritic spines in pyramidal neurons of the motor cortex in animal models should shed light on the mechanisms underlying the cortical synaptic abnormalities observed in PD patients with LID (Morgante et al., 2006; Suppa et al., 2011; Huang et al., 2012; Kishore et al., 2012).

The striatum of rodents receives excitatory inputs from two types of cortical pyramidal neurons in layer 5 of the cerebral cortex—those with intratelencephalic connections and those sending their axons to the brainstem via the pyramidal tract (Lei et al., 2004; Reiner et al., 2010). It has been demonstrated that the intratelencephalic (IT)-type neuron preferentially innervates striatal neurons of the contralateral and ipsilateral direct pathways, whereas the pyramidal tract (PT)-type neuron preferentially innervates striatal neurons of the ipsilateral indirect pathway (Reiner et al., 2010). The direct pathway plays a central role in the development of LID (Feyder et al., 2011). On the other hand, there is not sufficient evidence to support a role of the indirect pathway for LID (Cenci and Konradi, 2010). Thus, we investigated the morphological and electrophysiological changes in IT-type pyramidal neurons of M1 in rat models of PD and LID in the present study.

Materials and methods

The present study consists of two parts. The first part is the morphological examination of dendritic spine of IT-type neurons. The second part is the electrophysiological examination of IT-type neurons. The study designs are summarized in Fig. 1.

Experimental animals

Male Wistar rats (Japan Clea Co. Ltd, Tokyo, Japan) were housed in a temperature-controlled room (around 25 °C) with a 12-h day/night cycle, with free access to food and water. The experimental procedures employed in this study complied with the guidelines for animal research issued by the Physiological Society of Japan and by Hirosaki University School of Medicine, and all efforts were made to minimize the number of animals used and their suffering.

Creation of rat models

We prepared 14 6-hydroxydopamine (6-OHDA)-lesioned hemiparkinsonian rats (the PD model), 20 6-OHDA-lesioned hemiparkinsonian rats with chronic levodopa treatment (the LID model), 8 control rats with chronic levodopa treatment (levodopa-treated control) and 17 control rats with saline treatment (control) (Fig. 1).

At 10 weeks of age, rats underwent stereotactic infusion of 6-OHDA (the PD and LID models) or saline (levodopa-treated control and control) into the medial forebrain bundle (MFB) on the right side as previously described (Tanaka et al., 1999) (Fig. 1). The rats were pretreated with desipramine (25 mg/kg, intraperitoneally) 30 min before the injection into MFB to prevent denervation of noradrenergic neurons. A stainless steel needle (0.4 mm diameter) was inserted through a small burr hole on the right side of the skull and the needle tip was placed in the right MFB (4.5 mm posterior to the bregma, 1.2 mm lateral to the

sagittal suture, and 8.5 mm ventral to the dural surface) according to the atlas of Paxinos and Watson (1998). We injected 6-OHDA (8 mg/4 mL in saline with 0.01% ascorbic acid) over 4 min. After injection, the needle was left in place for 2 min to prevent backflow leakage from the site of injection.

To evaluate the extent of dopaminergic denervation, 2 weeks after the 6-OHDA injection, the rats were challenged with apomorphine (in saline with 0.1% ascorbic acid, 0.05 mg/kg, subcutaneously) (Fig. 1). The 6-OHDA-treated animals that made more than 20 contralateral (to the left) turns during a 5-min period between 15 and 20 min after apomorphine injection, indicating lack of dopaminergic function in the striatum (we previously showed that rats meeting this criterion had lost more than 99% of dopamine in the striatum; Maeda et al., 1999), were included in the present study. To confirm the dopaminergic denervation, brain sections of 6-OHDA-lesioned rats were immunostained with monoclonal antibodies against tyrosine hydroxylase (1:3000), using the avidin–biotin–peroxidase complex (ABC) method with a Vectastain ABC kit (Fig. 2). Dopaminergic denervation was mostly complete in the striatum, and was also found in M1 (Fig. 2). Four weeks after the apomorphine test, 6-OHDA-lesioned rats with dopaminergic deneravation and sham-operated rats received 50 mg/kg levodopa methyl ester with 12.5 mg/kg benserazide (the LID model and levodopa-treated control) or saline (the PD model and control), twice daily (morning and evening) for 14 consecutive days (Fig. 1). To evaluate the effects of levodopa, we measured the abnormal involuntary movement (AIM) score in the left side of the body on days 1, 4 and 10 (Cenci et al., 1998; Cenci and Lundblad, 2007) (Fig. 1). AIMs are considered to be comparable to LID in patients with PD (Cenci et al., 1998; Cenci and Lundblad, 2007). We observed and scored the rats every 20 min during the 2-h period following the injection of levodopa (Fig. 3). Scores are based on the duration and persistence of the dyskinetic behavior during the 1-min observation period. Movements were recognized as dyskinetic when they fulfilled the following criteria: (i) were induced by L-DOPA; (ii) affected the left side of the

body; (iii) were repetitive, purposeless and not ascribable to any normal behavioural pattern. AIMs were classified based on their topographic distribution into three subtypes: axial dystonia, i.e. twisted posturing of the neck and upper body to the left side; orolingual dyskinesia, i.e. stereotyped jaw movements and tongue protrusion to the left side; forelimb dyskinesia, i.e. repetitive rhythmic jerks or dystonic posturing of the left forelimb, and/or grabbing movement of the left paw. For each of these three subtypes, each rat was scored on a scale from 0 to 4 (1 = occasional; 2 = frequent; 3 = continuous but interrupted by sensory distraction; 4 = continuous, severe, not interrupted by sensory distraction) (Cenci et al., 1998). We assessed and summed the scores for the three AIM subtypes; limb, axial, and orolingual (Fig. 3).

Dendritic spine morphology

Eight 6-OHDA-lesioned hemiparkinsonian rats (the PD model), eight 6-OHDA-lesioned hemiparkinsonian rats with chronic levodopa treatment (the LID model), eight control rats with chronic levodopa treatment (levodopa-treated control) and eight control rats were used. To selectively label cell bodies of IT-type neurons in right M1, we stereotactically injected a retrograde tracer, Fast Blue, into the left dorsolateral striatum on day 11 of the drug treatment (Reiner et al., 2010) (Fig. 1). The stainless steel needle was inserted through a small burr hole on the left side of the skull, and the needle tip was placed in the left dorsal striatum (1.0 mm anterior to the bregma, 3.5 mm lateral to the sagittal suture, and 6.0 mm ventral to the dural surface). We injected Fast Blue (15 μg/1 μL in saline) over a 1-min period. After injection, the needle was left in place for 2 min to prevent backflow. Four days later, all rats were deeply anesthetized with sodium pentobarbital (Nembutal, >75 mg/kg, intraperitoneally), and intracardially perfused with 4% paraformaldehyde 12 h after the last treatment with levodopa or saline, and the brain was removed.

Serial 250-μm-thick coronal sections through M1 were prepared with the aid of a Microslicer (DSK DTK-1000; Dosaka EM, Kyoto, Japan). Individual sections were mounted between Millipore filters (AABG02500, Millipore Corporation, Billerica, MA, USA). The slice was then mounted in a Perspex dish on a fixed-stage microscope (Optiphot2-UD microscope; Nikon, Tokyo, Japan) and the labeled neurons in right M1 were observed under ultraviolet excitation (380–420 nm). Lucifer Yellow was injected into cell bodies of the Fast Blue-labeled neurons in right M1 under visual guidance with continuous current (up to 100 nA). Neurons were filled with Lucifer Yellow until their dendritic spines were sufficiently visible (Fig. 4A). The intracellular injections were performed as previous described (Buhl and Schlote, 1987; Elston and Rosa, 1997).

For confocal laser scanning microscopy, the sections were mounted onto slides and then coverslipped with Permount and SlowFade Gold Antifade Reagent (S36937, Invitrogen, Tokyo, Japan). The tissue was examined with a confocal microscope, and images were taken with a digital camera (C1si; Nikon). Yellow signals (515/530 nm) were acquired from each sample using 488 nm excitation. Fluorescence projection images of somata and dendritic fields were acquired with a 60× oil-immersion lens. Signal gain was adjusted so that the largest spine of the dendrite had the center of its head saturated with a yellow signal, but its edge was not saturated. We selected 5–10 cells for each rat, and 1–5 horizontally projecting dendrites from each cell. Horizontally projecting dendrites were selected to reduce errors. Then, we measured the density and size of spines on the basal dendrite, 50–100 μm distal to the cell body (Fig. 4B). Images of the spines in each dendrite were acquired with a 60× oil-immersion lens (5.0 zoom factor) with 0.0064 μm^2/pixel and taken at 0.25-μm focal steps. Image stacks were 3D-deconvoluted using the NIS-Elements software (Nikon) and volume rendered as 2D images to facilitate overview of the figures (Fig. 4C). In total, we measured 11427 spines from 203 neurons in 31 motor cortices. Each spine was manually traced. The average number of spines per 10 μm of linear dendritic length was expressed as the spine

density. We measured the cross-sectional area of the spine head in 2D reconstructed images. All spines were drawn, and no distinction was made between different spine types. All dendritic trees were reconstructed and all spines were drawn by the first author. Image analysis was performed using Image J (National Institutes of Health, Bethesda, MD, USA). For analyses, we selected intracellularly injected cells (Control: 51 cells; the PD model: 56 cells; the LID model: 49 cells; levodopa-treated control: 47cells) based on the following inclusion criteria: (1) presence of an unambiguous apical dendrite; (2) complete basal dendritic tree contained within the section; and (3) successfully filled, thereby revealing the complete basal dendritic arborization, as well as fine details, such as dendritic spines (Fig. 4A). From these cells, we drew and tallied individual dendritic spines in a blinded fashion.

Electrophysiological recordings

Six PD model rats, 12 LID model rats, and nine control rats were used in this study (Fig. 1). To selectively label the cell bodies of IT-type neurons in right M1, we injected the retrograde tracer DiI into the left dorsolateral striatum as described above. We performed brain slice preparation and whole-cell patch-clamp recordings 4–7 days after the DiI injection and 12 h after the last drug treatment. The procedures used for preparing rat brain slices containing M1 were similar to those described previously (Yamada et al., 2007). After the animals (18–20 weeks of age) were deeply anesthetized by halothane inhalation, they were decapitated, and brain sections were quickly placed in cold (4 °C) oxygenated artificial cerebrospinal fluid. The solution contained the following (in mM): 126 NaCl, 2.5 KCl, 1.25 NaH_2PO_4, 2 $MgSO_4$, 2 $CaCl_2$, 26 $NaHCO_3$ and 20 glucose. Coronal slices (300 μm thick) were cut using a vibratome (Vibratome VIB1500; Intracel, Royston, UK). Individual slices were allowed to recover at 34 °C for 1 h and then stored at room temperature.

Whole-cell patch-clamp recordings were performed from IT-type pyramidal neurons in right M1. The slices were transferred to the recording chamber and continuously perfused

with oxygenated artificial cerebrospinal fluid at 32–34 °C (2 ml/min). A constant temperature was maintained throughout each recording (Diamedical Co, Tokyo, Japan). DiI-labeled layer 5 pyramidal neurons in the primary motor cortex were identified visually with a 60× water immersion objective with infrared differential interference contrast (Eclipse E600FN; Nikon) and fluorescence optics via a cooled charge-coupled device camera (ORCA-R2; Hamamatsu Photonics, Hamamatsu, Japan.). To avoid photolytic damage, initial exposure to episcopic fluorescence illumination was brief (<10 s). Once the experiment was terminated, the neuron underwent a longer fluorescence exposure to ensure that it was labeled. Real-time images were contrast enhanced using HCImage software (Hamamatsu Photonics). Patch electrodes were fabricated from borosilicate capillary tubing of 1.5 mm diameter (GD-1.5, Narishige, Tokyo, Japan) using a Narishige PP-83 vertical puller (Narishige). The electrode resistance was in the range of 3–4.5 MΩ. The pipette solution contained (in mM): 150 cesium methanesulphonate, 0.1 EGTA, 10 HEPES, 3 $Mg(ATP)_2$ and 0.4 Na(GTP), pH 7.3 with CsOH. Recordings were made with a MultiClamp 700B amplifier (Molecular Devices, Sunnyvale, CA, USA) in conjunction with a Digidata 1322A digitizer (Molecular Devices) and Clampex software (pClamp 10, Molecular Devices). All signals were filtered at 2 kHz and sampled at 10 kHz. Whole-cell recordings were made using voltage-clamp mode (V_h = −70 mV) in the presence of a $GABA_A$ receptor antagonist, bicuculline methiodide, a $GABA_B$ receptor antagonist, CGP55845 (3 μM), and tetrodotoxin (TTX, 0.3 μM). Miniature excitatory postsynaptic currents (mEPSCs) were analyzed using the Mini Analysis program (Synaptosoft Inc., Decatur, GA, USA) with a threshold of 6 pA for event detection.

Drugs

The following drugs were used: Nembutal (Dainippon Sumitomo Pharma, Osaka, Japan), 6-OHDA, monoclonal anti-tyrosine hydroxylase (TH16), desipramine hydrochloride, apomorphine, desipramine hydrochloride, levodopa methyl ester hydrochloride, benserazide

hydrochloride, DiI, Lucifer Yellow, bicuculline methiodide (Sigma, San Diego, CA, USA), Vectastain ABC kit (Vector, Burlingame, CA, USA), Fast Blue (POL, Cat# 17740, Warrington, PA, USA), CGP55845 (Tocris, Ellisville, MO, USA), and TTX (Wako, Osaka, Japan).

Statistics

We calculated the average spine density of each neuron, and then the average for each rat. We calculated the average cross-sectional area of the three largest spines in each dendrite and the average for each neuron, as well as the average for each rat. The average spine densities and the average cross-sectional spine head areas of each rat were submitted to analyses. Statistical analyses were performed with statistical program R 3.0.2 (http://cran.ism.ac.jp/). A probability level of 5% ($P < 0.05$) was considered statistically significant. Variables are presented as mean ± SEM. The quantitative data were evaluated to determine whether they followed a normal distribution using the Shapiro–Wilk test. The spine densities, the cross-sectional area of the spine head and mEPSC amplitudes were analyzed using non-parametric tests (Kruskal–Wallis test, followed by the Steel–Dwass multiple comparison test), because the Shapiro–Wilk test indicated that the distributions were not normal ($P < 0.05$). The mEPSC frequencies were examined using parametric tests (one-way analysis of variance followed by the post-hoc Tukey–Kramer test), because the Shapiro–Wilk test indicated that the distributions were normal.

Results

Morphological changes in dendritic spines of IT-type neurons

The spine densities in IT-type neurons were not different among the four different groups (control: 8.1 ± 0.47; the PD model: 9.3 ± 0.25; the LID model : 9.0 ± 0.66; levodopa-treated

control: 12.0 ± 1.42) (Fig. 5A and 5B). Thus, neither dopaminergic denervation nor denervation plus levodopa treatment affected spine density in IT-type pyramidal neurons of right M1. Chronic levodopa treatment to normal rats (levodopa-treated control) did not change spine density.

Chronic levodopa treatment to normal rats (Levodopa-treated control) did not change the spine size. However, dopaminergic denervation (the PD model) increased the size of dendritic spines in IT-type neurons of right M1 when compred with controls. Additional chronic levodopa treatment to rats with dopaminergic denervation (the LID model) displayed further enlarged spines of these neurons when compared with the PD model (control: 0.31 ± 0.062 μm^2; the PD model: 0.41 ± 0.014 μm^2; the LID model: 0.48 ± 0.020 μm^2; levodopa-treated control: 0.31 ± 0.030 μm^2) (Fig. 5A and 5C). The size of dendritic spines in the LID was larger than those in the levodopa-treated control. Previous studies have shown that there are structural correlates of synaptic plasticity (Kasai et al., 2010a, 2010b). In general, spine size is correlated with the strength of synapses (Kasai et al., 2010a, 2010b). Thus, the enlargement of dendritic spines in IT-type neurons of the PD and LID models suggests that there are associated changes in the electrophysiological properties of these neurons. To examine this possibility, we further conducted the following electrophysiological experiments.

Electrophysiological changes in IT-type neurons

To evaluate the postsynaptic responsiveness of IT-type pyramidal neurons in the different groups of animals, mEPSCs (V_h: −70 mV) were compared among the three group (30 cells from nine control rats; 24 cells from 6 PD model rats; 39 cells from 12 LID model rats). The mEPSC frequencies were not significantly different among the three different groups (Fig. 6A and 6B) (control: 7.5 ± 0.54 Hz; the PD model: 7.8 ± 0.56 Hz; the LID model: 9.2 ± 0.52 Hz). The mEPSC amplitude in the LID model was significantly larger than in the control (Fig. 6A and 6C) (control: 10.0 ± 0.23 pA; the PD model: 10.9 ± 0.31 pA; the LID model: 11.4 ± 0.29

pA). There were no significant differences in control *vs* PD or PD *vs* LID. The increase in mEPSC amplitude suggests an increase in spine size (Segal, 2010). Thus, our electrophysiological results are compatible with our morphological findings.

Discussion

In the present study, we showed that IT-type pyramidal neurons in the primary motor cortex of the rat model of LID displayed an enlargement of dendritic spines and an increase in the amplitude of mEPSCs. These morphological and electrophysiological findings indicate that the IT-type pyramidal neurons in the dyskinesia-primed animals acquire supersensitivity to excitatory stimuli.

Morphological changes in dendritic spines of IT-type neurons

6-OHDA injection into the right MFB result in ipsilateral dopaminergic denervation of cerebral cortex and striatum on the right side (Fig.2). IT-type neurons project to the bilateral striatum whereas chronic levodopa treatment induces AIMs in the contralateral body to the 6-OHDA-lesioned side. This unilaterality of AIMs probably results from intact dopaminergic innervation in the left brain. Then, in the present study we analyzed IT-type neurons in the right motor cortex.

The destruction of nigral dopaminergic neurons, by itself or in combination with levodopa replacement therapy, has no effect on spine density in IT-type pyramidal neurons of M1 (Fig. 5A and 5B). This is compatible with previous results showing a preservation of spine density in the cortex after dopaminergic denervation (Miklyaeva et al., 2007; Wang and Deutch, 2008; Elsworth et al., 2012). Chronic levodopa treatment to normal rats was also without effects on spine density of the IT-type pyramidal neuron (Fig. 5A and 5B). However, there have been no published reports on changes in spine density of cortical neurons in

dyskinetic and levodopa-treated control animals. On the other hand, PD patients and animal models of PD display a spine loss in MSNs of the dorsal striatum (Stephens et al., 2005; Villalba and Smith, 2010).

Dopaminergic denervation increased the size of dendritic spines in IT-type neurons without induction of involuntary movements, and additional levodopa treatment further enhanced the enlargement of dendritic spines with induction of dyskinetic movements (Fig. 5C). However, levodopa treatment to normal rats was without effects on spine size and did not induce dyskinesia. These results suggest that the further enlargement of spines is a key element with regard to induction of dyskinesia.

Dendritic spine size is tightly correlated with the strength of the synapse (Matsuzaki et al., 2001) and is actively regulated during synaptic plasticity (Matsuzaki et al., 2004). LTP is accompanied by a persistent increase in spine size (Matsuzaki et al., 2004). The enlargement results from the polymerization of actin and the insertion of AMPA receptors in the dendritic spines (Bosch and Hayashi, 2012; Matsuzaki et al., 2004). These events lead to an increase in the sensitivity of postsynaptic sites to glutamate (Murakoshi and Yasuda, 2012). Conversely, the induction of LTD causes spine shrinkage (Zhou et al, 2004). The abnormal preservation of LTP-like plasticity in the motor cortex in patients with dyskinesia (Huang et al., 2012) represents supersensitivity of the motor cortex. With regard to LID, the enlargement of dendritic spines (Fig. 5A and 5C) would account for the lack of depotentiation-like cortical plasticity in patients with LID (Huang et al., 2012). In fact, using patch-clump recording the supersensitivity of IT-type neurons was confirmed in the LID model (Fig. 6A and 6C). Accordingly, the enlargement of spines could be a cellular mechanism that explains the abnormal plasticity in the motor cortex in PD patients with dyskinesia (Huang et al., 2012). However, a small but significant enlargement of spines in the PD model compared with controls (Fig. 5C) is not justified by the TMS results showing that patients with untreated PD lack LTP-like plasticity in the motor cortex (Morgante et al., 2006; Suppa et al., 2011;

Kishore et al., 2012). These abnormal plastic changes in untreated PD patients suggest that cortical neurons engaged in the plasticity become less sensitive (Holtmaat and Svoboda, 2009). Accordingly, we expected that spines of IT-type neurons in M1 would get shrunk in the PD model. It is unclear what mechanisms are involved in the enlargement of spines in the PD model. The effect of dopaminergic denervation on the whole motor cortex could be different from that on IT-type neurons. TMS reflects net functional alterations of the whole motor cortex, whereas we analyzed only morphological changes of IT-type neurons, one type of neurons in the motor cortex. Thus, enlargement of dendritic spines in IT-type neurons may not account for all electrophysiological changes in the motor cortex in PD. However, it is of note that dyskinetic rats displayed the further enlargement compared with the PD model rats (Fig. 5A and 5C). This indicates that the change in spine size is related to the development of LID and that the enlargement may underlie LID.

Dopaminergic neurons synapse onto dendritic spine in cerebral cortex (Goldman-Rakic et al., 1989). The dopaminergic projection to M1 comes from ventral tegmental area (Hosp et al., 2011). The MFB lesion by 6-OHDA induced mostly complete dopaminergic denervation in the striatum and cerebral cortex including M1 (Fig 2). It has been also shown that dopamine level in the cortex is reduced in rats with dopaminergic denervation induced by 6-OHDA injection into MFB (Navailles et al., 2011: Nandhu et al., 2011). Furthermore, levodopa-derived dopamine is released from serotonergic terminals into the cortex after levodopa administration in rats with dopaminergic denervation (Navailles et al., 2010). Consequently, dopaminergic denervation and the ensuing levodopa treatment could cause a marked alteration of dopamine-dependent gating effects at the spine. It remains unknown whether the plastic abnormalities in the motor cortex (Huang et al., 2012) are primary or secondary. They may arise from the direct pulsatile stimulation of dopamine receptors in the motor cortex after each levodopa treatment, or from indirect abnormal inputs from the basal ganglia that are associated with dyskinesia. A recent finding that abnormal cortical

oscillations are a key pathophysiological mechanism calls for a revision of the prevailing hypothesis that LID is linked to altered dopamine sensitivity only in the striatum (Halje et al., 2012).

We examined IT-type neuron in the present study, because it has been shown that IT-type neuron preferentially innervates striatal neurons of the direct pathway which plays a central role in the development of LID (Feyder et al., 2011; Reiner et al., 2010). However, this concept has been challenged (Ballion et al., 2008; Kress et al., 2013: Wall et al., 2013). Projections from IT-type and PT-type cortical neurons had a similar distribution in the direct and indirect pathway of medium spiny neurons in rodents (Kress et al., 2013: Wall et al., 2013), where as IT-type neurons provide the main excitatory input to direct and indirect pathway and the input of PT-type neuron is weaker (Ballion et al., 2008). At the present, specific IT-type innervation of striatal neurons giving rise to the direct pathway still is a matter of debate. We should bear in mind that demarcation of the IT-type and PT-type neurons is proposed in rodents, but not in primates (Lei et al., 2004; Reiner et al., 2010).

Electrophysiological characteristics of IT-type neurons

Based on the morphological changes in IT-type neurons of the PD and LID models, we explored the electrophysiological characteristics of these cells. We demonstrated a significant increase in the amplitude of mEPSCs in the LID model, but not in the PD model (Fig. 6C). Because mEPSC amplitude correlates with the size of dendritic spines (Segal, 2010), this increase in mEPSC amplitude in the LID model fits well with the observed enlargement of dendritic spines (Fig. 5C), and suggests that IT-type neurons acquire supersensitivity to glutamate in dyskinetic animals. In contrast, the frequency of mEPSCs is associated with spine number and the release of glutamate (Segal, 2010). The frequency of mEPSCs in IT-type neurons was unchanged in the PD and LID models (Fig. 6B). Accordingly, our

electrophysiological findings were compatible with the finding that spine density of IT-type neurons remained unchanged in the models (Fig. 5B).

While the PD model showed an enlargement of dendritic spines (Fig. 5C), the amplitude of mEPSCs was unchanged in the PD model compared with the control (Fig. 6C). These findings suggest that factors other than spine size contribute to glutamate sensitivity in IT-type neurons. The frequency and amplitude of AMPA receptor-mediated EPSCs are both increased in medium spiny neurons of the striatum in 6-OHDA-lesioned rats (Bagetta et al., 2012). Thus, electrophysiological characteristics of cortical neurons differ from those of striatal neurons after dopaminergic depletion.

Conclusion

The enlargement of dendritic spines and increase in amplitude of mEPSCs in IT-type pyramidal neurons of the primary motor cortex of dyskinetic rats suggest supersensitivity to glutamate of the neurons in the dyskinetic state. These findings provide insight that supersensitivity of IT-type neurons is relevant to pathogenesis of LID, and suggest that LID is linked to maladaptive motor information stored in the motor cortex.

Acknowledgments

The authors thank Ms. Saeko Osanai for her kind support in our study. This study was supported by a grant-in-aid for scientific research from the Ministry of Education, Culture, Sports, Science and Technology of Japan (No. 22590952) to Masahiko Tomiyama.

References

Bagetta, V., Sgobio, C., Pendolino, V., Del Papa, G., Tozzi, A., Ghiglieri, V., Giampà, C., Zianni, E., Gardoni, F., Calabresi, P., Picconi, B., 2012. Rebalance of striatal NMDA/AMPA receptor ratio underlies the reduced emergence of dyskinesia during D2-like dopamine agonist treatment in experimental Parkinson's disease. J Neurosci 32, 17921-31.

Ballion, B., Mallet, N., Bézard, E., Lanciego, JL., Gonon, F.,2008. Intratelencephalic corticostriatal neurons equally excite striatonigral and striatopallidal neurons and their discharge activity is selectively reduced in experimental parkinsonism. Eur J Neurosci 27, 2313-21.

Belujon, P., Lodge, DJ., Grace, AA., 2010. Aberrant striatal plasticity is specifically associated with dyskinesia following levodopa treatment. Mov Disord 25, 1568-76.

Bosch, M., Hayashi Y., 2012. Structural plasticity of dendritic spines. Curr Opin Neurobiol 22, 383-8.

Buhl, EH., Schlote, W.,1987. Intracellular lucifer yellow staining and electron microscopy of neurones in slices of fixed epitumourous human cortical tissue. Acta Neuropathol 75, 140-6.

Cenci, MA., Konradi, C., 2010. Maladaptive striatal plasticity in L-DOPA-induced dyskinesia. Prog Brain Res 183, 209-33.

Cenci, MA., Lee, CS., Björklund, A., 1998. L-DOPA-induced dyskinesia in the rat is associated with striatal overexpression of prodynorphin- and glutamic acid decarboxylase mRNA. Eur J Neurosci 10, 2694-706.

Cenci, MA., Lundblad, M., 2007. Ratings of L-DOPA-induced dyskinesia in the unilateral 6-OHDA lesion model of Parkinson's disease in rats and mice. Curr Protoc Neurosci. Chapter 9, Unit 9.25.

Elston, GN., Rosa, MG., 1997. The occipitoparietal pathway of the macaque monkey: comparison of pyramidal cell morphology in layer III of functionally related cortical visual areas. Cereb Cortex 7, 432-52.

Elsworth, JD., Leranth, C., Redmond, DE. Jr., Roth, RH., 2013. Loss of asymmetric spine synapses in prefrontal cortex of motor-asymptomatic, dopamine-depleted, cognitively impaired MPTP-treated monkeys. Int J Neuropsychopharmacol 16, 905-12.

Fabbrini, G., Brotchie, JM., Grandas, F., Nomoto, M., Goetz, CG., 2007. Levodopa-induced dyskinesias. Mov Disord 22, 1379-89.

Feyder, M., Bonito-Oliva, A., Fisone, G., 2011. L-DOPA-Induced Dyskinesia and Abnormal Signaling in Striatal Medium Spiny Neurons: Focus on Dopamine D1 Receptor-Mediated Transmission. Front Behav Neurosci 5, 71.

Goldman-Rakic, PS., Leranth, C., Williams, SM., Mons, N., Geffard, M., 1989. Dopamine synaptic complex with pyramidal neurons in primate cerebral cortex. Proc Natl Acad Sci U S A. 86, 9015-9.

Halje, P., Tamtè, M., Richter, U., Mohammed, M., Cenci, MA., Petersson, P., 2012. Levodopa-induced dyskinesia is strongly associated with resonant cortical oscillations. J Neurosci 32, 16541-51.

Holtmaat, A., Svoboda, K., 2009. Experience-dependent structural synaptic plasticity in the mammalian brain. Nat Rev Neurosci. 10,647-58.

Hosp, JA., Pekanovic, A., Rioult-Pedotti, MS., Luft, AR., 2011. Dopaminergic projections from midbrain to primary motor cortex mediate motor skill learning. J Neurosci 31:2481-7.

Huang, YZ., Rothwell, JC., Lu, CS., Chuang, WL., Chen, RS., 2012. Abnormal bidirectional plasticity-like effects in Parkinson's disease. Brain 134, 2312-20.

Kasai, H., Fukuda, M., Watanabe, S., Hayashi-Takagi, A., Noguchi, J., 2010a. Structural dynamics of dendritic spines in memory and cognition. Trends Neurosci 33, 121-9.

Kasai, H., Hayama, T., Ishikawa, M., Watanabe, S., Yagishita, S., Noguchi, J., 2010b. Learning rules and persistence of dendritic spines. Eur J Neurosci 32, 241-9.

Kishore, A., Popa, T., Velayudhan, B., Joseph, T., Balachandran, A., Meunier, S., 2012. Acute dopamine boost has a negative effect on plasticity of the primary motor cortex in advanced Parkinson's disease. Brain 135, 2074-88.

Kress, GJ., Yamawaki, N., Wokosin, DL., Wickersham, IR., Shepherd, GM., Surmeier, DJ., 2013. Convergent cortical innervation of striatal projection neurons. Nat Neurosci. 16, 665-7.

Lei, W., Jiao, Y., Del Mar, N., Reiner, A., 2004. Evidence for differential cortical input to direct pathway versus indirect pathway striatal projection neurons in rats. The Journal of neuroscience 24, 8289-8299.

Luft, AR., Schwarz, S., 2009. Dopaminergic signals in primary motor cortex. Int J Dev Neurosci. 27, 415-421.

Maeda, T., Kannari, K., Suda, T., Matsunaga, M., 1999. Loss of regulation by presynaptic dopamine D2 receptors of exogenous L-DOPA-derived dopamine release in the dopaminergic denervated striatum. Brain Res 817, 185-191.

Matsuzaki, M., Ellis-Davies, GC., Nemoto, T., Miyashita, Y., Iino, M., Kasai, H., 2001. Dendritic spine geometry is critical for AMPA receptor expression in hippocampal CA1 pyramidal neurons. Nat Neurosci 4, 1086-92.

Matsuzaki, M., Honkura, N., Ellis-Davies, GC., Kasai, H., 2004. Structural basis of long-term potentiation in single dendritic spines. Nature 429, 761-6.

Miklyaeva, EI., Whishaw, IQ., Kolb, B., 2007. A golgi analysis of cortical pyramidal cells in the unilateral parkinson rat: absence of change in the affected hemisphere vs hypertrophy in the intact hemisphere. Restor Neurol Neurosci 25, 91-9.

Morgante, F., Espay, AJ., Gunraj, C., Lang, AE., Chen, R., 2006. Motor cortex plasticity in Parkinson's disease and levodopa-induced dyskinesias. Brain 129,1059-69.

Murakoshi, H., Yasuda, R., 2012. Postsynaptic signaling during plasticity of dendritic spines. Trends Neurosci 35,135-43.

Nandhu, MS., Paul, J., Kuruvilla, KP., Malat, A., Romeo, C., Paulose, CS., 2011. Enhanced glutamate, IP3 and cAMP activity in the cerebral cortex of unilateral 6-hydroxydopamine induced Parkinson's rats: effect of 5-HT, GABA and bone marrow cell supplementation. J Biomed Sci. 18.1, 5.

Navailles, S., Bioulac, B., Gross, C., De. Deurwaerdère, P., 2010. Serotonergic neurons mediate ectopic release of dopamine induced by L-DOPA in a rat model of Parkinson's disease. Neurobiol Dis 38, 136-43.

Navailles, S., Bioulac, B., Gross, C., De. Deurwaerdère, P., 2011. Chronic L-DOPA therapy alters central serotonergic function and L-DOPA-induced dopamine release in a region-dependent manner in a rat model of Parkinson's disease. Neurobiol Dis. 41, 585-90.

Paxinos, G., Watson, C., 1998. The rat brain in stereotaxic coordinates. Academic Press, San Diego, CA.

Picconi, B., Centonze, D., Håkansson, K., Bernardi, G., Greengard, P., Fisone, G., Cenci, MA., Calabresi, P., 2003. Loss of bidirectional striatal synaptic plasticity in L-DOPA-induced dyskinesia. Nat Neurosci 6, 501-6

Picconi, B., Paillé, V., Ghiglieri, V., Bagetta, V., Barone, I., Lindgren, HS., Bernardi, G., Angela Cenci, M., Calabresi, P., 2008. L-DOPA dosage is critically involved in dyskinesia via loss of synaptic depotentiation. Neurobiol Dis 29, 327-35

Picconi, B., Bagetta, V., Ghiglieri, V., Paillè, V., Di Filippo, M., Pendolino, V., Tozzi, A., Giampà, C., Fusco, FR., Sgobio, C., Calabresi, P., 2012. Inhibition of phosphodiesterases rescues striatal long-term depression and reduces levodopa-induced dyskinesia. Brain 134, 375-87.

Reiner, A., Hart, NM., Lei, W., Deng, Y., 2010. Corticostriatal projection neurons - dichotomous types and dichotomous functions. Front Neuroanat 4, 142

Rothwell, J., 2007. Transcranial magnetic stimulation as a method for investigating the plasticity of the brain in Parkinson's disease and dystonia. Parkinsonism Relat Disord 13, 417-20.

Segal, M., 2010. Dendritic spines, synaptic plasticity and neuronal survival: activity shapes dendritic spines to enhance neuronal viability. Eur J Neurosci 31, 2178-84.

Stephens, B., Mueller, AJ., Shering, AF., Hood, SH., Taggart, P., Arbuthnott, GW., Bell, JE., Kilford, L., Kingsbury, AE., Daniel, SE., Ingham, CA., 2005. Evidence of a breakdown of corticostriatal connections in Parkinson's disease. Neuroscience 132, 741-54.

Suppa, A., Marsili, L., Belvisi, D., Conte, A., Iezzi, E., Modugno, N., Fabbrini, G., Berardelli, A., 2011. Lack of LTP-like plasticity in primary motor cortex in Parkinson's disease. Exp Neurol 227, 296-301.

Tanaka, H., Kannari, K., Maeda, T., Tomiyama, M., Suda, T., Matsunaga, M.,1999. Role of serotonergic neurons in L-DOPA-derived extracellular dopamine in the striatum of 6-OHDA-lesioned rats. Neuroreport. 10, 631-4.

Villalba, RM., Smith, Y., 2010. Striatal spine plasticity in Parkinson's disease. Front Neuroanat 4,133.

Wall, NR., De. La. Parra, M., Callaway, EM., Kreitzer, AC., 2013. Differential innervation of direct- and indirect-pathway striatal projection neurons. Neuron 79, 347-60.

Wang, HD., Deutch, AY., 2008. Dopamine depletion of the prefrontal cortex induces dendritic spine loss: reversal by atypical antipsychotic drug treatment. Neuropsychopharmacology 33, 1276-86.

Yamada, J., Furukawa, T., Ueno, S., Yamamoto, S., Fukuda, A.,2007. Molecular basis for the GABAA receptor-mediated tonic inhibition in rat somatosensory cortex. Cereb Cortex 17,1782-7.

Zhou, Q., Homma, KJ., Poo, MM., 2004. Shrinkage of dendritic spines associated with long-term depression of hippocampal synapses. Neuron 44, 749-57.

Figure legends

Fig. 1. Time chart and experimental design of the study. We injected 6-hydroxydopamine (6-OHDA) or saline into the medial forebrain bundle to make hemiparkinsonian (LID: levodopa-induced dyskinesia model; PD: Parkinson disease model) or sham-operated rats (Levodopa-treated control: LTC; control: C), respectively. The number indicates number of weeks post-6-OHDA lesion. Dopaminergic denervation in 6-OHDA-injected rats was confirmed by apomorphine test. LID and LTC started to receive daily levodopa treatment and PD and C satarted to receive daily saline. Arrows indicate abnormal involuntary movement rating sessions. Closed and open triangles indicate the days of the tracer injection and sacrifice, respectively.

Fig. 2. Thyrosine hydroxylase immunohistochemistry in a section through anterior striatum from a 6-hydroxydopamine-lesioned rat. (A) Dopamine denervation was evident in the right (R) hemisphere, especially in the striatum. Scale bar = 2.5 mm. (B) Higher magnification view of the area indicated by white asterisk in (A) showing a dopaminergic denervation in the right primary motor cortex. Scale bar = 50 μm. (C) Higher magnification view of the area indicated by black asterisk in (A) showing intact dopaminergic innervation in the left primary motor cortex. Scale bar = 50 μm.

Fig. 3. The abnormal involuntary movement (AIM) scores of unilaterally 6-hydroxydopamine-lesioned rats treated with levodopa (levodopa induced dyskinesia model model ; LID) or levodopa treated control (LTC) on day 1, day 7, day 14 of treatment. The scores are the total scores of the three AIM subtypes; limb, axial, and orolingual (Cenci and Lundblad, 2007). The total score of the three AIMs was significantly increased in the LID model along with levodopa treatment (Kruskal–Wallis test followed by the Steel–Dwass

multiple comparison test: ** $P < 0.001$ vs Day 1, $^{\#\#}$ $P < 0.001$ vs Day 7). LTC showed no AIMs. LID, levodopa-induced dyskinesia model; LTC, levodopa-treated control model.

Fig. 4. (A) Representative confocal images of a IT-type pyramidal neuron in the primary motor cortex. IT-type neurons were filled with Lucifer Yellow until their dendritic spines became sufficiently visible. We randomly selected several cells for each tissue slice, and several horizontally projecting dendrites for each cell. Arrows: basal dendrites; Arrowhead: apical dendrite; Scale bar = 50 μm. (B) Dendritic spines on the dendrite, 50–100 μm distal from the cell body, were examined. Scale bar = 50 μm. (C) Higher magnification view of the area indicated by asterisk in (B) showing a basal dendrite 50–100 μm distal from the soma. Small green dots along the basal dendrite represent dendritic spines. The scale bar = 5 μm.

Fig. 5. Morphological evaluation of spines on basal dendrites. (A) Representative confocal microscopy images of dendritic spines of IT-type neurons in 250-μm-thick motor cortical tissue preparations from control, the Parkinson Disease model (PD), the levodopa-induced dyskinesia model (LID) and levodopa-treated control (LTC). Scale bar = 5 μm. (B) No significant changes in spine density among the four groups. (C) The spine was enlarged in the PD and LID models, but the enlargement was significantly greater in the LID model. (*$P < 0.05$, **$P < 0.01$, Kruskal–Wallis test followed by the Steel–Dwass multiple comparison test). C, control; PD, Parkinson's disease model; LID, levodopa-induced dyskinesia model; LTC, levodopa-treated control model.

Fig. 6. Miniature excitatory synaptic currents (mEPSCs) in the primary motor cortex from control, the Parkinson Disease model (PD), the levodopa-induced dyskinesia model (LID).

The frequency of mEPSC was unchanged (A and B) whereas the amplitude of mEPSC was significantly greater in LID model rats than in control rats (A and C). (**$P < 0.01$, Kruskal–Wallis test followed by the Steel–Dwass multiple comparison test).

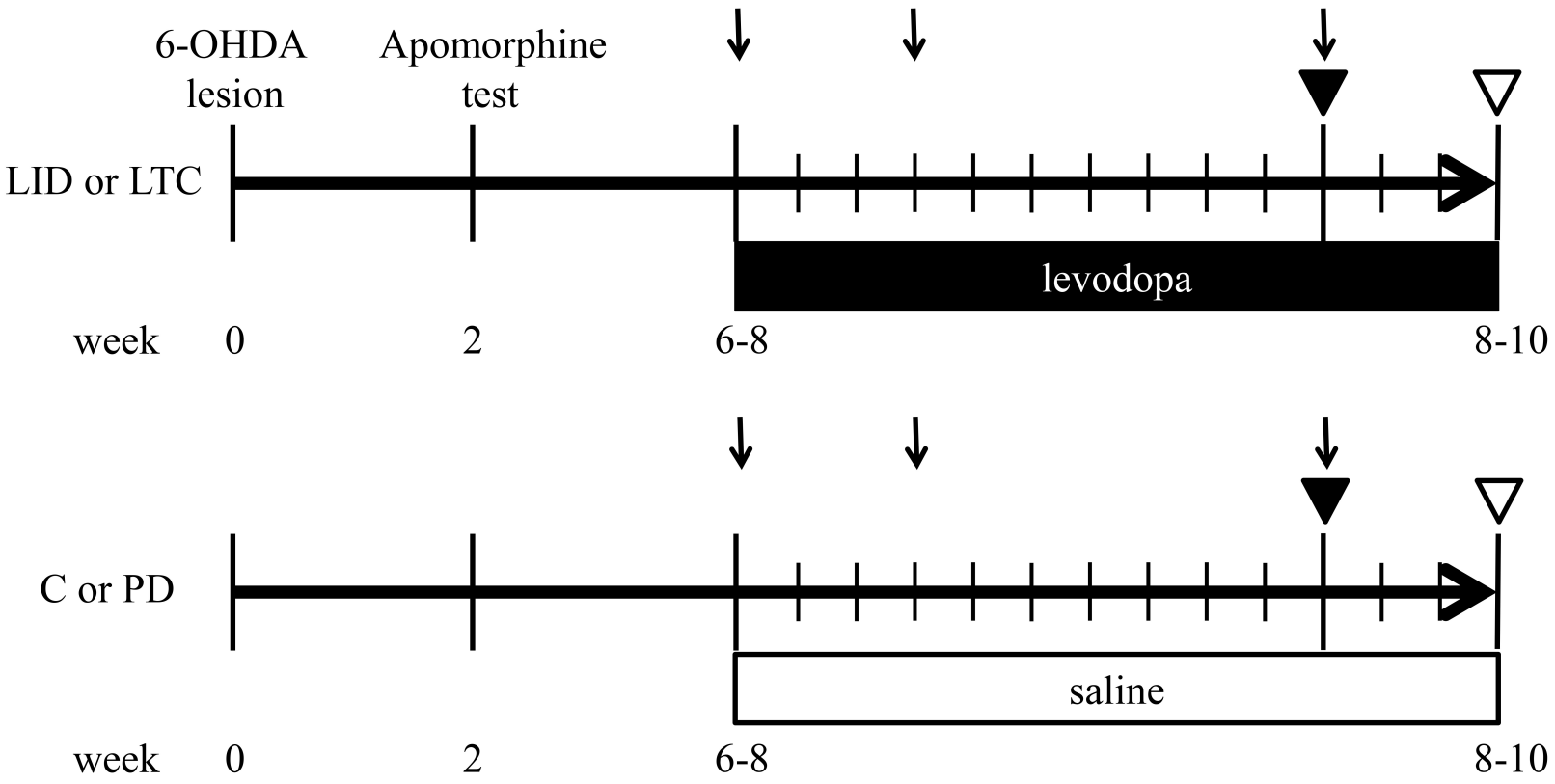
6-OHDA lesion
Apomorphine test
LID or LTC
levodopa
week
0
2
6-8
8-10
C or PD
saline
week
0
2
6-8
8-10

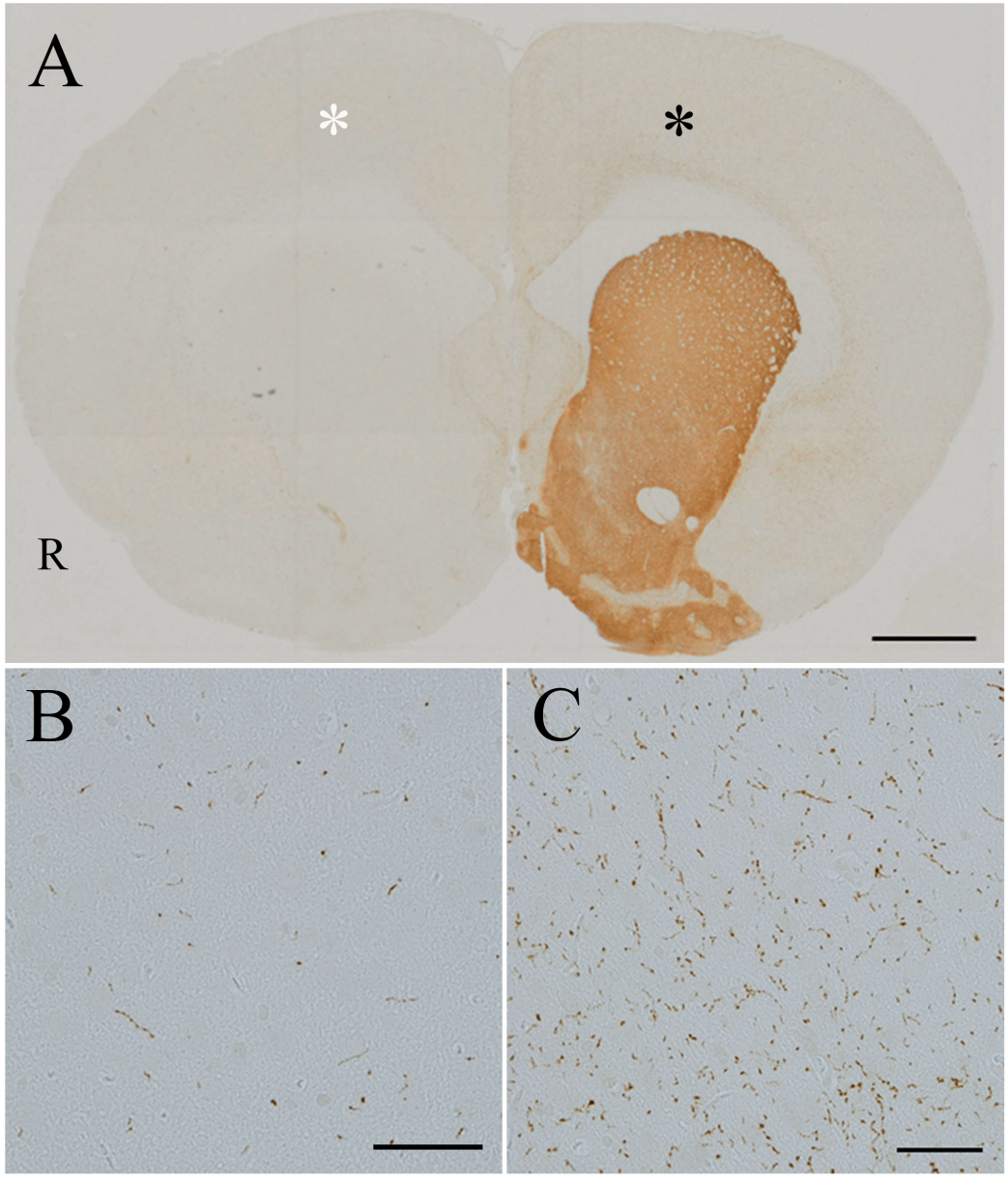
A
*
*
R
B
C

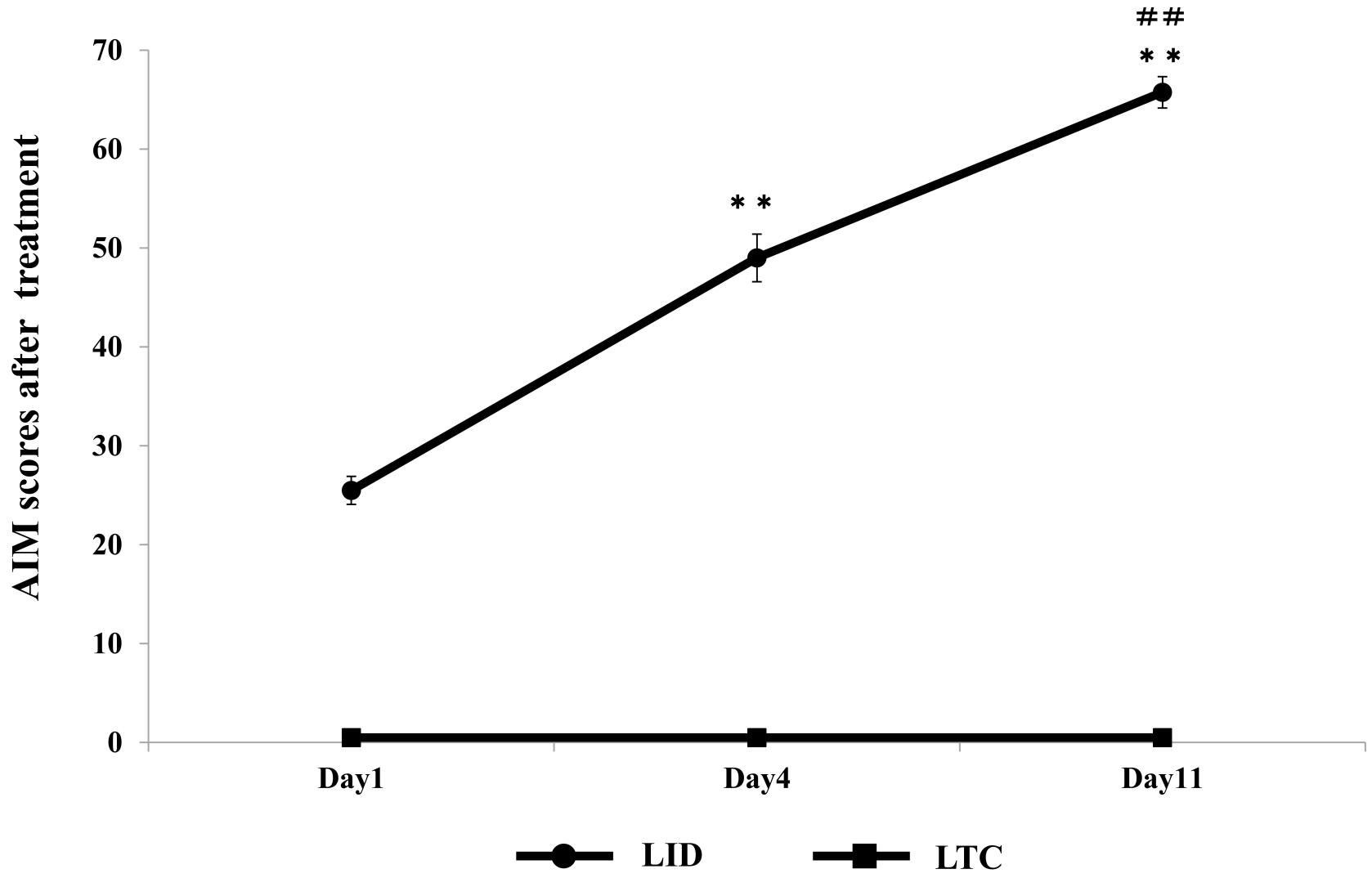
AIM scores after treatment
70
60
50
40
30
20
10
0
Day1
Day4
Day11
* *
* *
##
LID
LTC

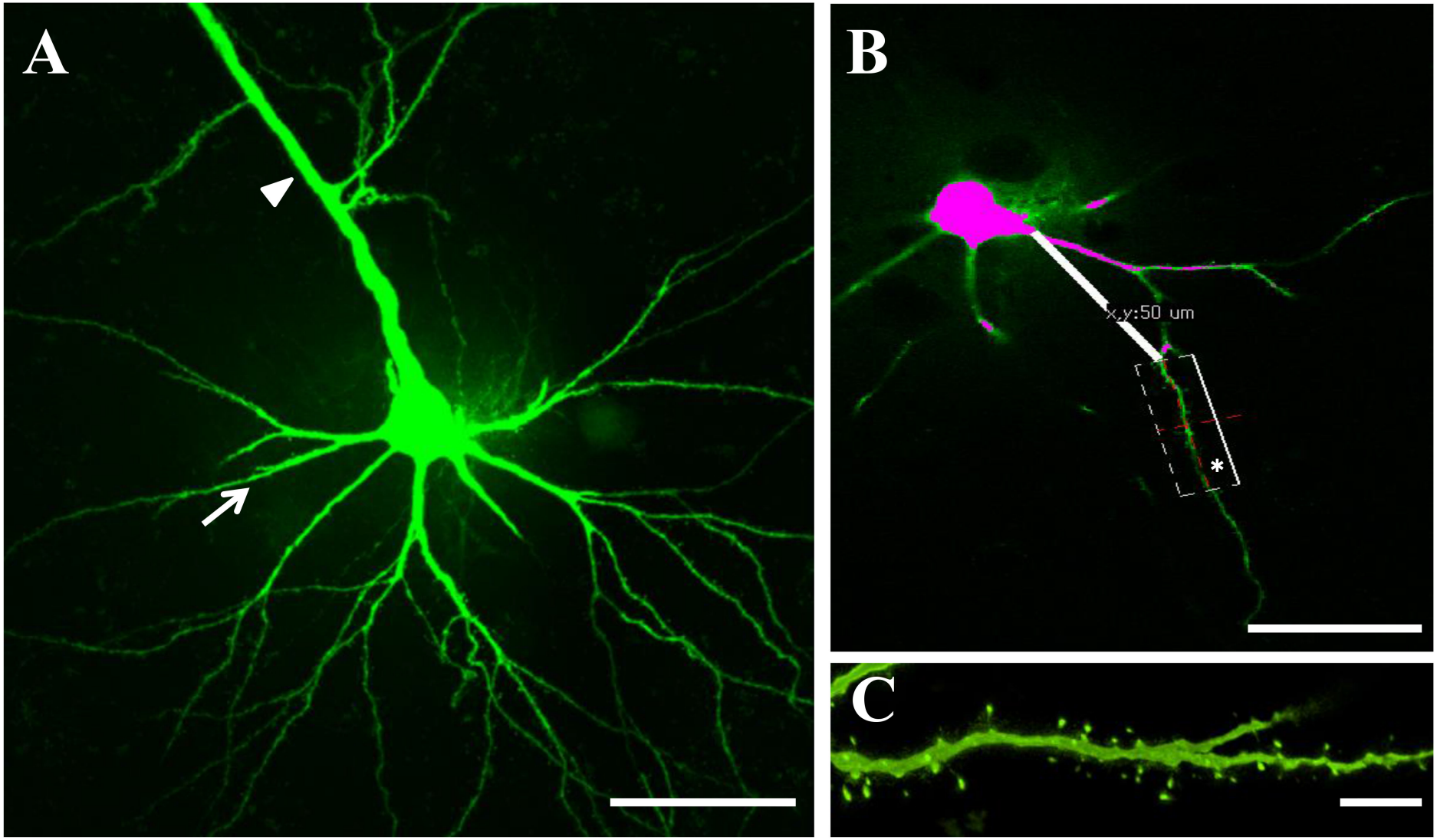
A
B
x,y:50 um
*
C

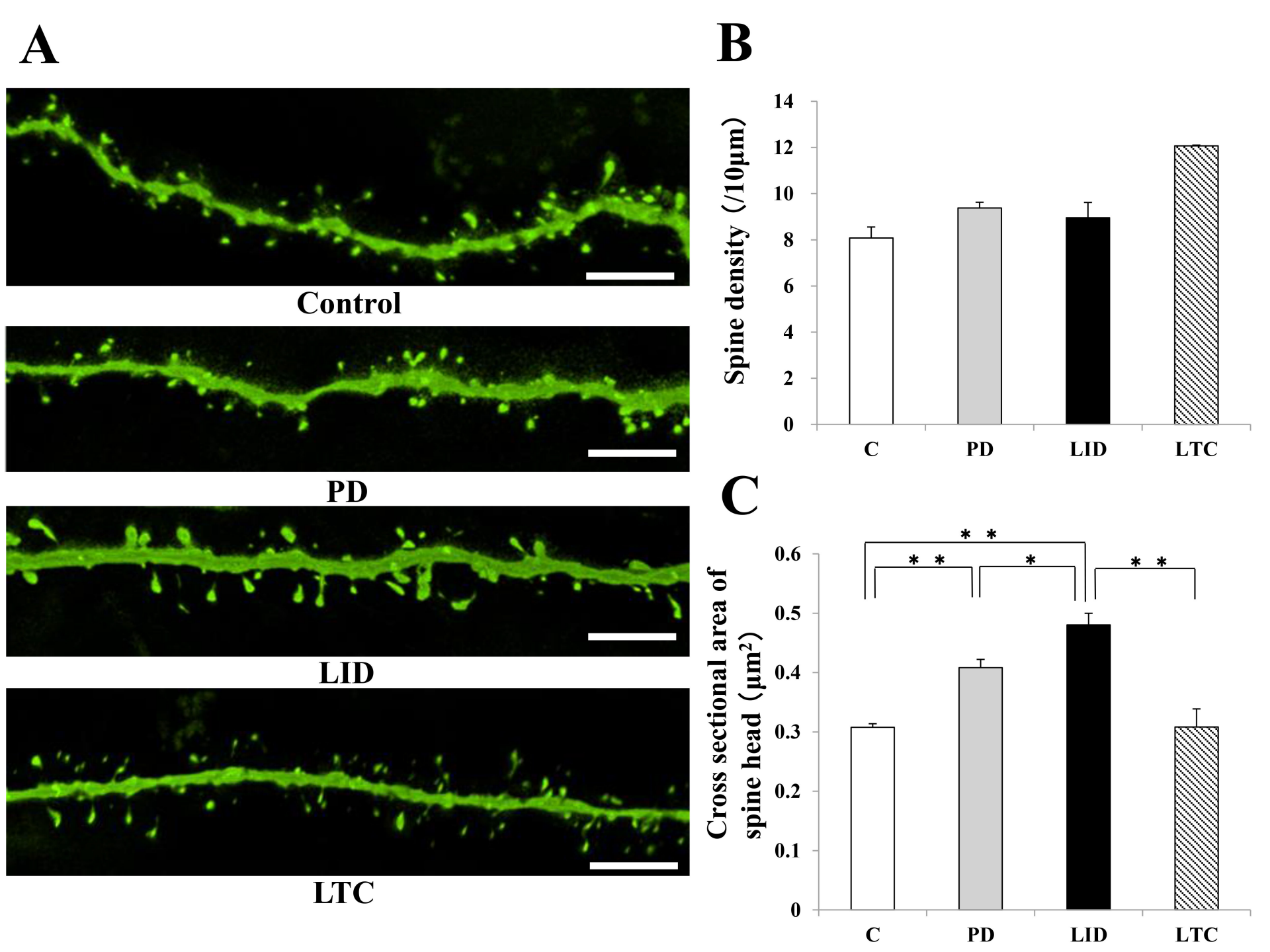
A
Control
PD
LID
LTC
B
Spine density (/10μm)
14
12
10
8
6
4
2
0
C
PD
LID
LTC
C
Cross sectional area of spine head (μm²)
0.6
0.5
0.4
0.3
0.2
0.1
0
* *
* *
*
* *
C
PD
LID
LTC

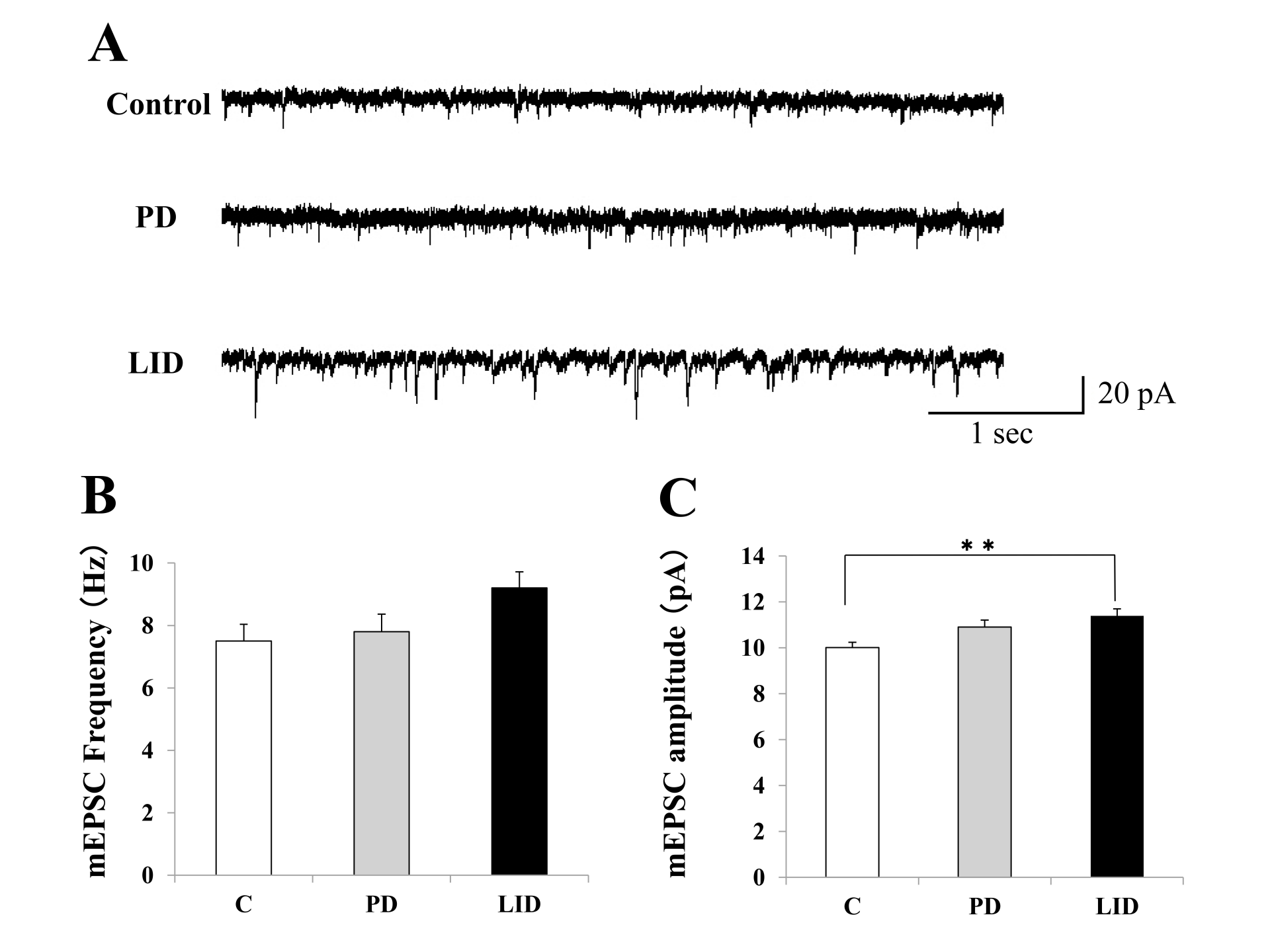
A
Control
PD
LID
20 pA
1 sec
B
mEPSC Frequency (Hz)
0
2
4
6
8
10
C
PD
LID
C
mEPSC amplitude (pA)
0
2
4
6
8
10
12
14
* *
C
PD
LID